Supplemental Materials

SUPPLEMENTAL EXPERIMENTAL PROCEDURES

Animals and Immunizations

Indian-origin rhesus macaques (n=4) were primed with 4 mg of plasmid DNA expressing transmitted-founder (TF) CH505 gp145 by electroporation with a BTX electroporator (DNA-EP) at weeks 0 and 4. Five weeks later, rhesus macaques were boosted with wildtype CH505 TF gp140, and the Envs from weeks 53, 78 and 100 post-transmission in this sequential order. The full Env names are week 53.16, 78.33, 100.B6 which includes the clone identification number. Env proteins were formulated with Poly ICLC (Hiltonol®, Oncovir) immediately before administration. Protein boosts were administered every six weeks and immunogenicity assessed at 24 hours, 7 days, and 14 days post immunization. A draining inguinal lymph node was biopsied at the end of the study following the 6^{th} immunization (**Table S1**).

New Zealand white rabbits (n=4) were immunized 6 times with 100 µg of CH505 TF ch.SOSIPs. CH505 TF ch.SOSIPs were formulated with Poly ICLC (Hiltonol®, Oncovir) just prior to immunization. Intramuscular immunizations occurred every 4 weeks and immunogenicity was assessed 10 days post-immunization. All animal procedures were IACUC approved prior to performance. All animals were cared for in an AAALAC-accredited facility in accordance with NIH guidelines.

CH103 UCA homozygous HC only (V_HDJ_H-only) KI mice, with homozygously knocked-in CH103 UCA V_HDJ_H rearrangements ($V_HDJ_H^{+/+}$ KI strains), or CH103 UCA heterozygous “HC only” KI mice, with heterozygously

knocked-in CH103 UCA V_HDJ_H rearrangements ($V_HDJ_H^{+/-}$ KI strains), were generated on the C57BL/6 background as previously reported (Williams et al., 2017), based on previously described Ig site-directed gene-targeting techniques (Chen et al., 2013; Verkoczy et al., 2011; Verkoczy et al., 2010). Briefly, for all vaccinations with CH103 HC only KI strains 8-12 wk, equal gender-distributed mice (n=4) were immunized up to seven times with 25 μg of the CH505 TF Env gp120 protein formulated with 5 μg of the TLR4 agonist-based, IDRI proprietary adjuvant system GLA-SE. Immunizations were performed via intraperitoneal injections (200 uL) administered every 21 days. Control groups were administered in parallel with saline, or in some cases, with 5 μg of GLA-SE (adjuvant only) Blood samples were collected 10 days after each immunization in order to isolate plasma for immunogenicity assays.

Flow cytometry single cell sorting of mouse memory B-cells

Single cell sorting of activated (class-switched, memory) B-cells from CH103 UCA HC KI only strains was performed as previously described (Williams et al, submitted). Briefly, single suspensions of total splenocytes were stained using anti-B220, anti-CD19, anti-CD93, anti-CD38, anti-IgD, and anti-IgG1,G2a/2b, G3. IgG+ memory B cells were visualized by first gating on lymphocyte singlets, followed by exclusion of LIVE/DEAD® Near IR stained cells (to discriminate live from dead cells), subsequent gating for CD19+B220+ (total B-cells), and finally, gating for CD38+IgG+IgD- (class-switched, memory B-cells). CH103 lineage specificity of the IgG+ memory B-cell subset was detected by using the combination of tetramerized, AlexaFluor 647 and Brilliant Violet 421-tagged HIV-1 Env gp120 wild type or mutant CH505 TF-derived gp120 proteins

(TF-BV421 and Δ371 TF-AF647, respectively), with differential binding to the former, but not the latter, indicating enrichment for CH103 bnAb lineage-specific binding to the Env CD4bs. TF Env+ switched memory (Near IR-, CD19+B220+CD38+IgG+IgD-) B-cells induced in Env-immunized mice, and for comparison, total IgG+ switched B-cells from control (saline or "adjuvant alone")-immunized mice, were sorted using a FACSAria II (BD Biosciences, San Jose, CA) into BioExpress 96 well plates (T-3085-1) containing 20 µl of SuperScript® III reverse transcriptase buffer (LifeTech). Sorted plates were frozen in a dry ice ethanol bath and stored at -80°C until further processed.

PCR isolation and immunogenetic analysis of mouse HC and LC rearrangements

HC/LC rearrangement pairs were recovered from single sorted memory B-cells based on previous methods (Williams et al., 2017). Briefly, cDNAs from individual 96 plate's wells were generated by RT synthesis using SuperScript® III Reverse Transcriptase and random primers as per manufacturer's instructions (LifeTech), followed by two rounds of PCR amplification using Ig reverse and forward primer sets. For isolation of KI-derived HC rearrangements, forward primers (outer and nested) were used that were specific for either the common J558 H10 leader peptide in the KI HC expression cassette or human V_H4-59. Parallel PCR amplifications using degenerate leader V_H family-specific primer mixtures were also used to detect mouse endogenous HC rearrangements. For all HC rearrangements isolated (KI or endogenous), reverse primer mixtures of Cγ1,Cγ2b, Cγ2c, Cγ3, and Cα-specific primers (40) were used to specifically isolate activated (i.e. class-switched) B-cells. Likewise, for isolation of LC rearrangements, forward degenerate leader Vκ and Vλ primer mixtures, in

combination with reverse Cκ and Cλ-specific primers, respectively, were used to detect endogenous LC kappa or LC lambda rearrangements.

Cloned PCR products were then purified and directly sequenced in both orientations (GeneWiz) using published primers and V, D, and J segment usage was determined by querying amplified sequences to both the original CH103 HC UCA rearrangement and relative to C57BL/6 Ig germline sequences in the IMGT database using IMGT/HighV-QUEST search software. CH103 UCA KI, murine endogenous V_HDJ_H, or the various hybrid rearrangements described in this study were all sequenced in both directions and analyzed for SHMs relative to germline, using DNASTAR MegAlign Pro multiple sequence alignment software.

Expression of HC and LC rearrangements as full-length IgG1 rmAbs

Expression plasmids (encoding selected natural pairs of HC/LC rearrangements from memory B-cells of vaccinated CH103 HC only KI mice) were used for Recombinant monoclonal antibody (mAb) production in human embryonic kidney cell lines (ATCC, Manassas, VA) (Liao et al., 2009) via small-scale transfection. To obtain larger quantities for full characterization, purified mAbs were then generated, dialyzed against PBS, analyzed, and stored at 4°C, all as previously described (Liao et al., 2013).

Direct ELISAs

ELISAs were performed as previously described (Saunders et al., 2017). Nunc-absorp plates were coated with 2 µg/mL of envelope in sodium bicarbonate buffer overnight at 4 °C. The plates were blocked with SuperBlock and incubated with serially diluted plasma. Binding antibodies were detected with HRP labeled

IgG antibodies. HRP was detected with 3,3',5,5'-Tetramethylbenzidine. Binding titers were analyzed as area-under-curve of the log transformed concentrations.

Recombinant monoclonal antibodies were screened by ELISA for reactivity with wildtype HIV-1 Envs and their corresponding gp120 proteins with mutations in the CD4bs (Δ371Ile), V1V2 glycan (N156/160Q) or V3 glycan (N332A). MPER reactivity was determined with peptides derived from gp41.

Competition ELISAs

Plasma blocking of PG9 binding to CH505 TF gp120 Env was measured by ELISA as previously described (Hulot et al., 2015). To determine plasma blocking activity, CH505 TF gp120 was incubated for 90 min with plasma prior to the addition of biotinylated PG9. PG9 binding was determined with HRP linked-streptavidin.

TZM-bl neutralization assay

Plasma from all animal models and purified antibodies were screened for neutralization using the TZM-bl assay, performed as previously described (Li et al., 2005).

HIV-1 Env Peptide Array

Peptide arrays were performed as previously described (Shen et al., 2017), with minor modifications. Briefly, array slides were provided by JPT Peptide Technologies GmbH (Germany) by printing a library of peptides onto epoxy glass slides (PolyAn GmbH, Germany). The library contains overlapping peptides (15-mers overlapping by 12) covering 6 full-length gp160 consensus sequences (clade A, B, C, and D, group M, CRF1, and CRF2) and gp120 sequences of 6 vaccine strains (MN, A244, Th023, TV-1, ZM651, 1086C). Three

identical subarrays were blocked for 1 h, followed by a 2-h incubation with 1:50-diluted serum samples and a subsequent 45-min incubation with anti-monkey IgG conjugated with AF647 (Jackson ImmunoResearch, PA). Array slides were scanned at a wavelength of 635 nm using an InnoScan 710 scanner (InnopSys, Denmark) and images were analyzed using Mapix V8.1.1.

Autoantigen ELISA

Autoantibodies were measured by the FDA-approved AtheNA Multi-Lyte® ANA II Test Kit from Zeus Scientific, Inc. per the manufacturer's instructions.

Activation-induced marker (AIM) assay

The AIM assay was performed as previously described (Havenar-Daughton et al., 2016). Briefly, rhesus macaque PBMC and lymph node cell suspensions (10^6 cells) were cultured for 18 hours at 37°C/5% CO_2 with no exogenous stimulation or with gp140 stimulation (5 µg/ml CH505 Week 100.B6 gp140C Env protein and 0.5 µg/ml of each 15-mer peptide of an 11-residue overlapping peptide pool spanning CH505 Env). As a positive control for T cell activation, some cells from each animal were stimulated with the superantigen *Staphylococcus aureus* Enterotoxin B (1 µg/ml). When cell numbers permitted, replicates of each condition were performed. Following stimulation, cells were labeled with antibodies to the following surface antigens: CD3 (SP34-2), CD4 (OKT4), biotin CXCR5 (MU5UBEE) followed by detection with Streptavidin PE-Cy7, PD-1 (EH12.2H7), OX40 (L206), and CD25 (BC96). Flow cytometric data were acquired on a LSRII using FACSDIVA software (BD Biosciences) and were analyzed with FlowJo software (FlowJo). Frequencies of Env-specific Tfh cells

were calculated as the percentage of Tfh cells that were $OX40^{+}CD25^{+}$ when gated as shown in Supplemental Figure 6.

Design of CH505 chimeric, stabilized Env trimer immunogens

The design of HIV-1 gp140 SOSIP proteins from clade C viruses is challenging, and in particular CH505 SOSIP proteins were low yield and unstable (Liu et al., 2015; Zhou et al., 2017). Trimer stability was improved by grafting most of the CH505 gp120 onto the BG505 gp41 forming a chimeric SOSIP (Zhou et al., 2017). The CH505 sequence was fused to BG505 sequence in the alpha 5 helix. We introduced I203C and A433C mutations (Kwon et al., 2015) and E64K and A316W mutations (de Taeye et al., 2015), which have been shown to keep SOSIP trimers in the pre-CD4 bound state. The SOSIP trimers were purified by PGT145 positive selection and Superdex200 size exclusion chromatography as stated below. See also **Figure S1**.

HIV-1 Envelope production and purification

HIV-1 gp120 and gp140 proteins were produced in 293F cells and purified by *Galanthus nivalis* lectin as previously described (Saunders et al., 2017). CH505 TF ch.SOSIP trimers were transfected in 293F cells using 293fectin. Each liter of 293F cells received 650 µg of plasmid DNA encoding the SOSIP trimer and 150 µg of furin-encoding plasmid DNA. Six days post transfection the supernatant was cleared of cells, concentrated, and subjected to PGT145 affinity chromatography. PGT145 columns were made by conjugating 100 mg of PGT145 to 10 mL of sepharose fast flow resin (GE Healthcare). Trimeric envelope was purified in 10 mM Tris pH8, 500 mM NaCl on a HiLoad

Superdex200 16/600 column (GE Healthcare). All proteins were snap-frozen and stored at -80°C.

Negative stain electron microscopy and single particle 2D class averaging

Samples for negative stain electron microscopy were prepared by diluting protein to 20 µg/ml in HMK100 buffer [50mM HEPES, 100mM KAc, and 5mM MgAc (pH 7.6)]. Ten microliters of protein were added to a carbon-coated grid. The sample was removed and the grid was stained with 5 drops of 2% uranyl acetate. Imaging was performed using a Philips 420 electron microscope at 49000x magnification.

Class averaging of the single particle images collected by negative stain EM was conducted using the EMAN2 program (Tang et al., 2007). At least 10,000 particles were picked using the automated particle picking function in EMAN2. All picked particles were used to prepare initial 2D class averages. Refinement was accomplished by manually removing classes composed of artifact or background particles, and rerunning the 2D class averaging.

Antibody-SOSIP biolayer interferometry

Biolayer interferometry was performed as previously described (Alam et al., 2017). Antibodies were immobilized to anti-Fc sensor tips and incubated with SOSIP trimers solutions for 400 seconds.

SUPPLEMENTAL TABLES

Table S1. Env name and recombinant form used for rabbit and rhesus macaque vaccination.							
Animal model	**Immunization number**						
	1	**2**	**3**	**4**	**5**	**6**	**7**
Rabbits (n=4)	**Unstabilized CH505 TF ch.SOSIP**	**Unstabilized CH505 TF ch.SOSIP**	**Unstabilized CH505 TF ch.SOSIP**	**Unstabilized CH505 TF ch.SOSIP**	**Unstabilized CH505 TF ch.SOSIP**	**Unstabilized CH505 TF ch.SOSIP**	
Rabbits (n=8)	**Stabilized CH505 TF ch.SOSIP**	**Stabilized CH505 TF ch.SOSIP**	**Stabilized CH505 TF ch.SOSIP**	**Stabilized CH505 TF ch.SOSIP**	**Stabilized CH505 TF ch.SOSIP**	**Stabilized CH505 TF ch.SOSIP**	
Rhesus macaques (n=4)	**CH505 TF gp145**	**CH505 TF gp145**	**CH505 TF gp140C**	**CH505 week 53.16 gp140C**	**CH505 week 78.33 gp140C**	**CH505 week 100.B6 gp140C**	**CH505 week 100.B6 gp140C**

Table S1. Env name and recombinant form used for rabbit and rhesus macaque vaccination. Related to Figure 1 and 2. The immunogens used in each vaccination study at each immunization are listed. The gp145 immunizations were administered as DNA plasmid followed by electroporation. All other immunizations were protein mixed with adjuvant delivered intramuscularly. Numbers after the decimal place in the Env name indicate clone identification number. TF, transmitted founder.

Table S2 Distribution of long HCDR3-generating atypical hybrid HC rearrangements expressed by CH103 UCA "HC only" KI memory B-cells.					
CH103 UCA "HC only" KI genotype	**Treatment Group (# of mice)**	**# of atypical rearrangement products / total memory B-cells cloned**	**Type of atypical HC rearrangement product (length of HCDR3)[a]**		
			mVD-hVDJ hybrid (23-24 aa)	**mVD-hDJ hybrid (DD fusion-like) (20-22 aa)**	**mV-hVDJ hybrid (V_H replacement-like) (17-19 aa)**
$V_HDJ_H^{+/-}$	**Control (Saline-injected X5) (*n*=1)**	**2/68**	**2**	**0**	**0**
	CH505-immunized (TF Env gp120 in GLA-SE X5) (*n*=2)	**4/73**	**2**	**1**	**1**
$V_HDJ_H^{+/+}$	**Controls (Saline-injected X5) (*n*=2)**	**1/31**	**0**	**1**	**0**
	CH505-immunized (TF Env gp120 in GLA-SE X5) (*n*=2)	**16/81**	**3**	**12**	**1**

Table S2. Distribution of long HCDR3-generating atypical hybrid HC rearrangements expressed by CH103 UCA "HC only" KI memory B-cells.

Related to Figure 3. Indicated in the 3rd column are the frequencies of all atypical HC rearrangement products recovered from the single Env-specific IgG^+ sorted memory B-cell pool in saline injected vs. CH505-immunized heterozygous and homozygous CH103 UCA "HC only" KI mice. Shown in columns 4-7 are the types of atypical HC rearrangement products identified and their relative distributions across genotypes and treatment groups. [a]Reported HCDR3 lengths are based on Kabat nomenclature.

Table S3. Immunogenetics of V1V2$^+$ 23aa HCDR3-bearing human recombinant mAbs derived from single IgG$^+$ memory B-cell VDDJ/VJ pairs of TF-immunized CH103 UCA homozygous "HC only" KI mice.

mAb ID	Heavy Chain							Light Chain			
	mV_H	mD_H	hD_H	hJ_H	% V_H SHM	Top human V_H orthologue(s)	% homology	mV_L	mJ_L	Top human V_L orthologue(s)	% homology
5808-1A4	1-22*01	1-1*01	3-16*01	4*02	8.2	1-3*01 1-69*01	67.3 67.0	Vκ6-14*01	Jκ1*01	κ1-17	65.0
5808-1A6	1-22*01	1-1*01	3-16*01	4*02	7.1	1-8*01 1-2*02	65.3 64.3	Vκ6-14*01	Jκ1*01	κ1-17	66.3
5808-1D5	1-22*01	1-1*01	3-16*01	4*02	8.2	1-8*01	66.3	Vκ6-14*01	Jκ1*01	κ1-6	66.0
5808-1G2	1-22*01	1-1*01	3-16*01	4*02	7.1	1-8*01	63.3	Vκ6-14*01	Jκ1*01	κ1-17	66.3
5808-1G4	1-22*01	1-1*01	3-16*01	4*02	3.1	1-2*02	66.3	Vκ6-14*01	Jκ1*01	κ1-6	65.0
5808-1G5	1-22*01	1-1*01	3-16*01	4*02	5.1	1-8*01 1-2*02	65.3 64.3	Vκ6-14*01	Jκ1*01	κ1-17	66.0

Table S3. Immunogenetics of V1V2$^+$ 23aa HCDR3-bearing human recombinant mAbs derived from single IgG$^+$ memory B-cell VDDJ/VJ pairs of TF-immunized CH103 UCA homozygous "HC only" KI mice. Related to Figure 4. Shown are the V, D, and J mini-gene segments expressed by each mAb (with human, knock-in-derived segments in red lettering and endogenous, murine-derived ones in blue lettering, respectively). Also shown in column 5 is the % amino acid mutation in mouse V_H1-22 (relative to the germline), as well as the putative human V_H and V_L orthologues (or closest homologues) of translated murine V_H1-22 and Vκ6-14 (columns 5 and 9, respectively), and their percent protein identities (columns 6 and 10, respectively). The three antibodies

produced in high quantities (used for further characterization as shown in Figures 6B-C) are bolded.

SUPPLEMENTAL FIGURES

Figure S1

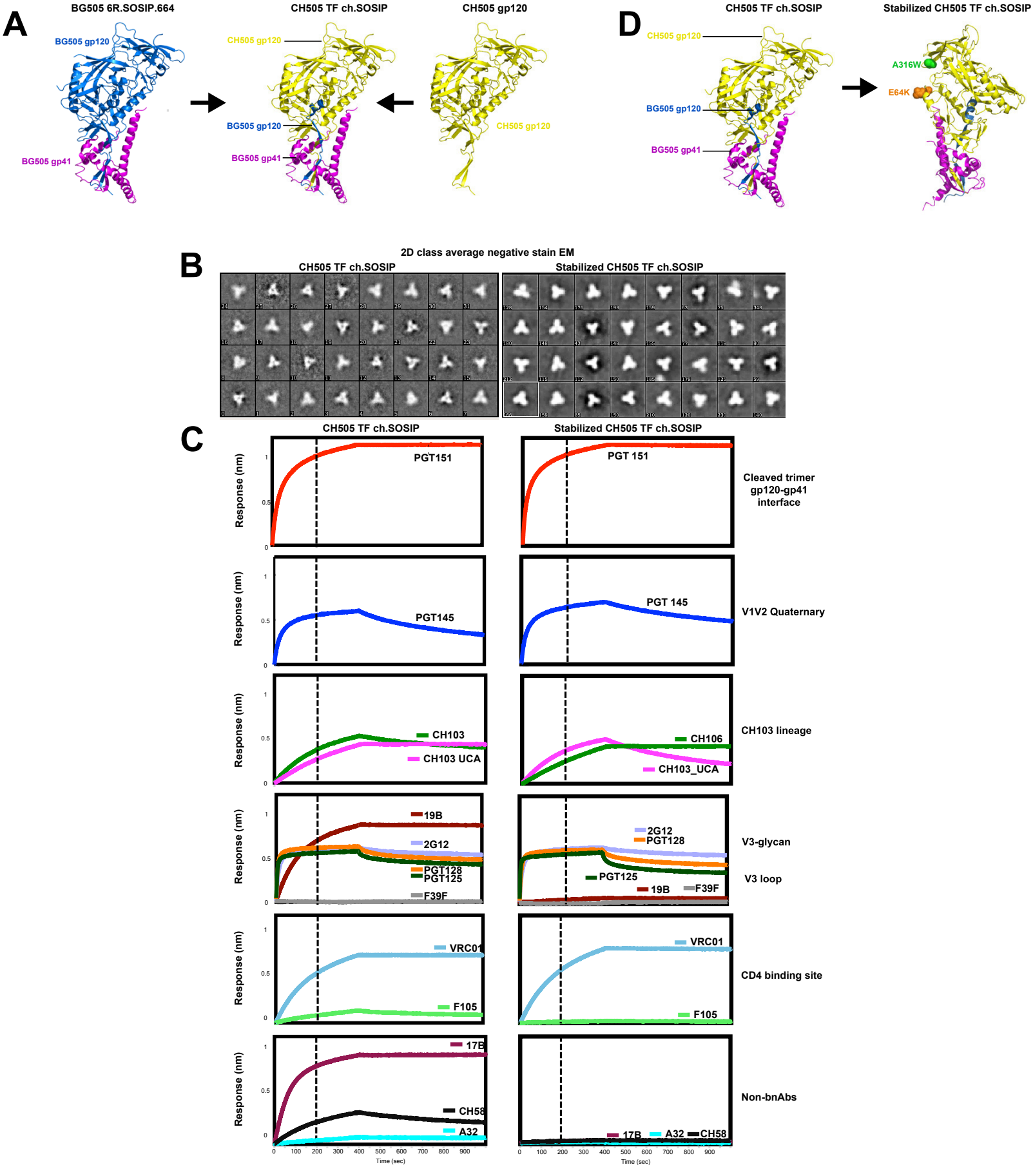

Figure S1. Stabilization of soluble trimers eliminates non-neutralizing antibody binding, but retains bnAb and CH103 UCA binding. Related to Figure 1.

(A) Design of unstabilized CH505 chimeric SOSIP (ch.SOSIP) trimers.

(B) This unstabilized CH505 TF chimeric SOSIP (ch.SOSIP) formed trimeric Envelope protein as shown by negative stain electron microscopy. 2-D class averages of negative stain electron microscopy (EM) of purified unstabilized (left) and stabilized (right) CH505 ch.SOSIP trimers.

(C) Antigenicity of unstabilized and stabilized ch.SOSIP trimers as measured by biolayer interferometry. These trimers were antigenic for trimer-specific interface, trimer-specific V1V2, CD4 binding site, and V3 glycan bnAbs. However, the CH505 TF ch.SOSIP trimer also bound antibodies that lacked neutralization breadth, and thus was not a mimic of the native trimer on the virus surface. Antigenically stabilized CH505 TF ch.SOSIP shown in **(D)** maintained binding by bnAbs, but eliminated binding by poorly neutralizing antibodies. The Env appeared to be in the pre-CD4 bound state as the CD4-induced epitope was not present based on a lack 17B binding and the V3 loop was unexposed as evidenced by a lack of 19B binding. Representative curves are shown for each antibody indicated.

(D) Stabilization of the CH505 ch.SOSIP trimers by introducing A316W and E64K mutations. The CH505 TF ch.SOSIP envelope with E64K and A316W mutations, termed stabilized CH505 TF ch.SOSIP, formed trimers shown in (**B**).

Figure S2

A

Purified immunoglobulin neutralization titer (IC50; ug/mL)			
Rabbit ID	Study week	TRO.11 Tier 2	SVA NA
S402	21	276	>317

B

Purified immunoglobulin neutralization titer (IC50; ug/mL)			
Macaque ID	Study week	TRO.11 Tier 2	SVA NA
6207	30	30	>950
	36	269	>875

C

	SVA-MLV	TRO.11	TRO.11 N279A	TRO.11 N280D	TRO.11 G458Y	TRO.11 N160K	TRO.11 N295V	TRO.11 N332A	TRO.11 N625A	TRO.11 N88A
Sample ID	NA	WT	CD4bs	CD4bs	CD4bs	V1V2 glycan	V3 glycan	V3 glycan	MPER	Fusion peptide
S402 wk21	<20	160	253	169	76	118	59	49	111	198
CH01-31	>25	0.24	>25	18	3.4	0.24	0.34	0.36	0.27	0.18

D

S402 serum neutralization (ID50, reciprocal dilution)								
Rabbit ID	Study week	TRO.11	TRO.11 N332A		Ce1176_A3	Ce1176_A3 N332A	25710-2.43	25710-2.43 N332A
S402	21	160	49		450	209	446	194

E

	SVA-MLV	TRO.11	TRO.11 N160K	TRO.11	TRO.11 N332A	TRO.11 IMC	TRO.11 IMC N276D
Sample ID	NA	WT	V1V2 glycan	WT	V3 glycan	WT	CD4bs
6207 wk30 plasma	<20	149	32	330	95	282	209
6207 wk36 plasma	<20	129	70	246	128	240	153
PG9	>25	>5	>5	NT	NT	NT	NT
PG16	>25	1.4	>10	NT	NT	NT	NT
CH103	>25	3.34	3.45	2.6	4.6	>11.5	3.3
CH235	>25	16.18	22.2	11	11	14	15
PGT128	>25	0.02	0.02	<0.011	20	NT	NT
CH31	>25	NT	NT	NT	NT	0.32	21
HJ16	>25	NT	NT	NT	NT	0.15	>25

F

	SVA-MLV	CH0505 TF	CH505 TF N160Q	CH505 TF N160A	CH0505 TF N301A	CH0505 TF N334A	CH0505 TF	CH0505 TF N280D	CH0505 TF G458Y
Sample ID	NA	WT	V1V2 glycan	V1V2 glycan	V3 glycan	V3 glycan	WT	CD4bs	CD4bs
6207 wk30 plasma	<20	126	50	44	72	145	206	220	1101
6207 wk36 plasma	<20	112	63	59	59	144	204	178	875
PG9	>25	0.26	>5	>5	NT	NT	NT	NT	NT
PG16	>25	0.05	>10	>10	NT	NT	NT	NT	NT
CH103	>25	2.9	2.5	1.8	1.6	3.2	1.9	1.2	5.8
CH235	>25	0.58	0.55	0.54	0.32	0.7	0.3	>25	0.1
VRC01	>25	NT	NT	NT	NT	NT	0.1	>25	>25
PGT128	>25	>19	>10	>10	>10	>10	NT	NT	NT

Figure S2 Purified immunoglobulin from a vaccinated rabbit or macaque mediates heterologous tier 2 neutralization. Related to Figure 1 and 2.

(A) Total gamma immunoglobulin was purified from (A) rabbit S402 plasma after the final immunization. Neutralization activity was examined in the TZM-bl assay and titers are indicated as IC50 in μg/mL of purified IgG.

(B) Total immunoglobulin was purified from rhesus macaque 6207 using anti-kappa and anti-lambda resin after the last two immunizations (week 30 and 36). Neutralization activity was examined in the TZM-bl assay and titers are indicated as IC50 in μg/mL of purified Ig. Positive neutralization titers are highlighted in orange.

(C) Epitope mapping of HIV-1 neutralization responses in S402 sera. In the TZM-bl assay a panel of TRO.11 viruses with mutations in known bnAb epitopes were tested for neutralization sensitivity to rabbit S402 serum. Serum was obtained from the end of the vaccination regimen (study week 21). The reciprocal serum ID50 titers are color-coded as in Figure 1.CH01 and CH31 pooled together were used as a positive control and IC50 in μg/mL is color-coded as >25, white; 25-1, yellow; 1-0.01, orange; <0.01, red.

(D) Rabbit S402 serum neutralization of multiple heterologous tier 2 viruses is partially dependent on asparagine 332 (N332). Neutralization activity against three wildtype tier 2 viruses and their corresponding viruses with an alanine substitution at position 332. Neutralization titers are shown as reciprocal dilution of S402 serum from the end of the vaccination regimen (study week 21). The titers are color-coded as in Figure 1.

(E, F) Epitope mapping of HIV-1 neutralizing antibodies in RM 6207 plasma. (E) TRO.11 and (F) CH505 TF viruses were mutated at known bnAb epitopes and neutralization was tested in the TZM-bl assay. The ability of the plasma from week 30 and 36 to neutralize the wildtype (WT) and mutant viruses are shown. The mutant viruses were assayed in batches and the wildtype virus was included in each assay. Plasma titers are shown as ID50 in reciprocal dilution of plasma. Monoclonal antibodies were used as positive controls for the mutations. Their neutralization titers are shown as IC50 in μg/mL and color-coded as in (C).

Figure S3

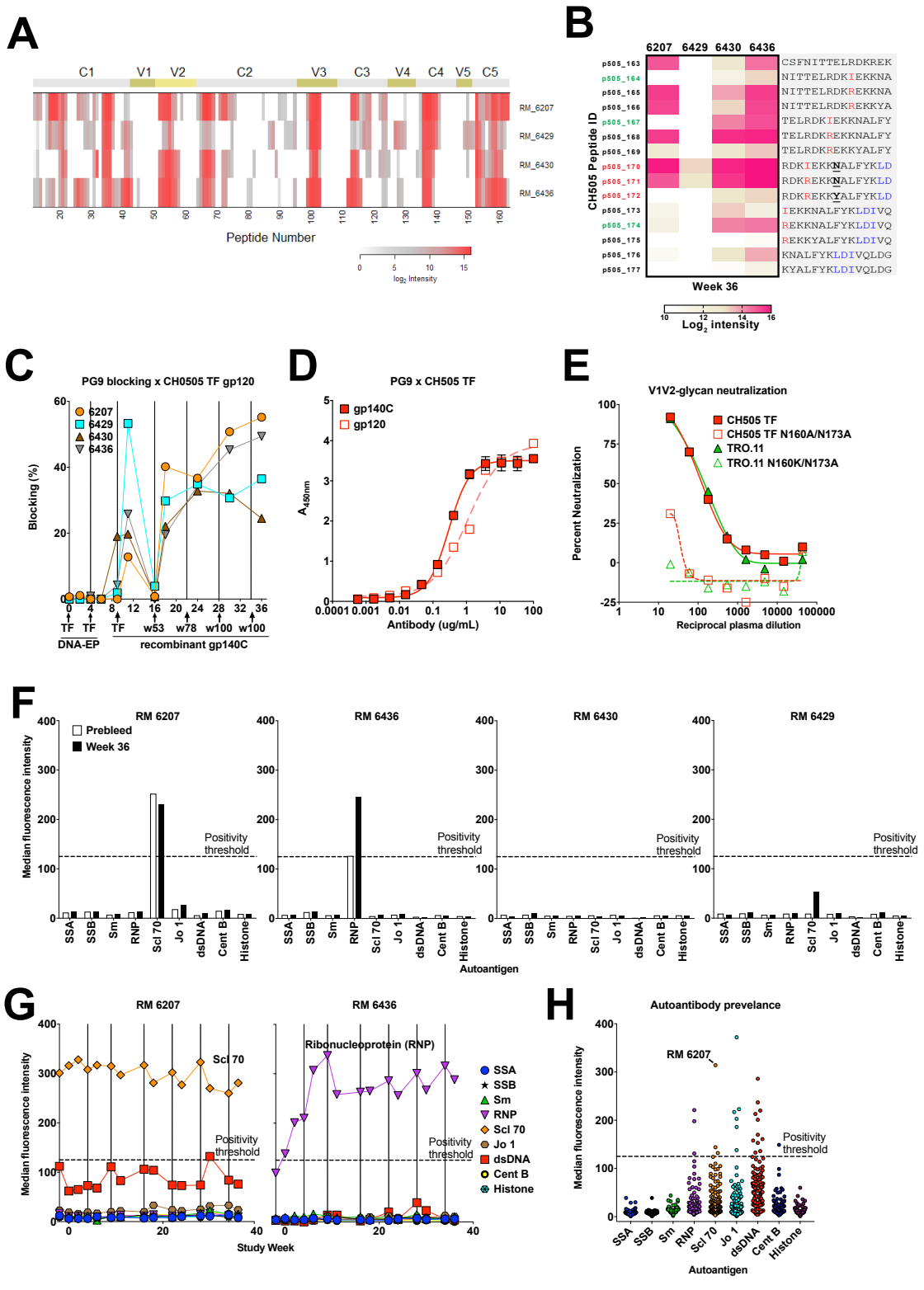
A
C1
V1
V2
C2
V3
C3
V4
C4
V5
C5
RM_6207
RM_6429
RM_6430
RM_6436
Peptide Number
log2 Intensity
B
6207 6429 6430 6436
CH505 Peptide ID
Week 36
Log2 intensity
C
PG9 blocking x CH0505 TF gp120
Blocking (%)
DNA-EP
recombinant gp140C
D
PG9 x CH505 TF
gp140C
gp120
A450nm
Antibody (ug/mL)
E
V1V2-glycan neutralization
CH505 TF
CH505 TF N160A/N173A
TRO.11
TRO.11 N160K/N173A
Percent Neutralization
Reciprocal plasma dilution
F
RM 6207
RM 6436
RM 6430
RM 6429
Prebleed
Week 36
Median fluorescence intensity
Positivity threshold
SSA
SSB
Sm
RNP
Scl 70
Jo 1
dsDNA
Cent B
Histone
Autoantigen
G
RM 6207
RM 6436
Scl 70
Ribonucleoprotein (RNP)
Study Week
H
Autoantibody prevalance
RM 6207

Figure S3. Characterization of V1V2-glycan and autoreactive antibody responses in macaque 6207 plasma. Related to Figure 2.

(A) HIV-1 Envelope peptide array binding for week 36 plasma IgG antibodies. The intensity of binding is for any clade, defined as the highest binding to a single peptide of any clade at each peptide position, and is indicated by the shade of red color per the key below. Each row is an individual RM.

(B) CH505 peptide binding intensity by plasma IgG for each macaque. Intensity of binding is indicated per the key below. The peptide sequence is shown on the right. Peptide identification (ID) is shown on the left side of the grid. Peptides in green indicate peptides bound by 6430 and 6436 but not the macaque that made bnAbs. Note the change in binding with a I169R (peptide 164 versus 165; and peptide 167 versus 168) or a N173Y (peptide 171 versus 172) change in the peptide sequence.

(C) Plasma blocking of PG9 binding to CH505 TF gp120. PG9 binding to CH505 gp120 was determined in the presence and absence of plasma. Each curve represents the macaque identified in the legend. The arrows on the x-axis indicate vaccination timepoints.

(D) ELISA binding of V1V2 glycan bnAb PG9 to the vaccine immunogens.

(E) Neutralization titers for RM6207 plasma against wildtype CH505 and TRO.11 (solid lines) and viruses with mutations in the PG9 epitope in the V1V2 loop (dotted lines).

(F) Plasma IgG binding to autoantigens as measured by the Athena assay. Open bars are before vaccination and filled bars represent binding at week 36 (2

weeks post final immunization). Binding greater than the dashed line indicates positive values.

(G The autoantibodies kinetics throughout vaccination for the two macaques (6207 and 6436) with detectable autoantibodies in the plasma at week 36. Each curve represents a unique autoantibody. Binding greater than the dashed line indicates positive values.

(H) The seroprevalence of autoantibodies in 114 nonhuman primates measured in the Athena assay. 6207 showed the highest Scl70 binding.

Figure S4

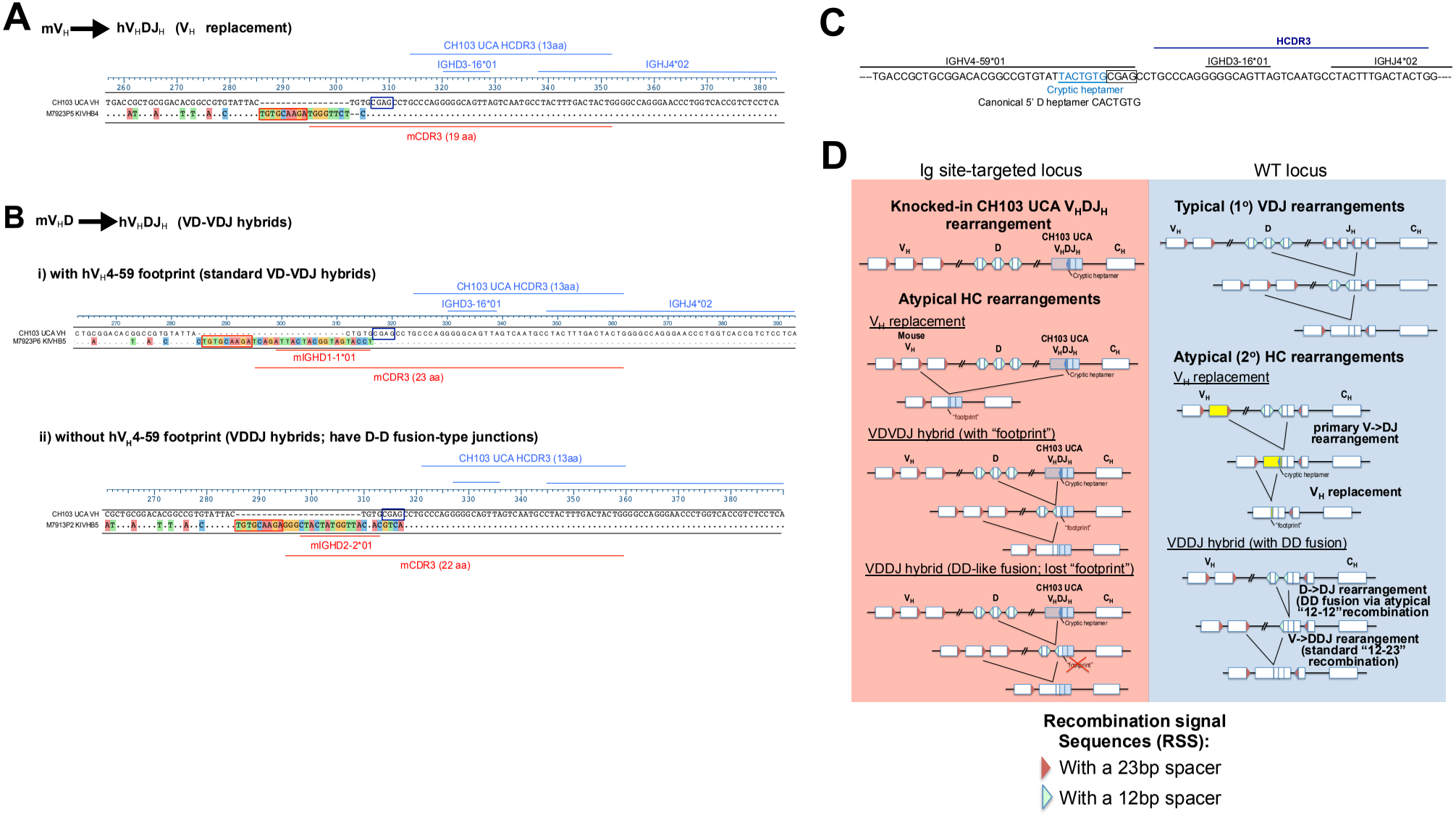
A
mV$_H$ → hV$_H$DJ$_H$ (V$_H$ replacement)
CH103 UCA HCDR3 (13aa)
IGHD3-16*01
IGHJ4*02
CH103 UCA VH
M7923P5 KIVHB4
mCDR3 (19 aa)
B
mV$_H$D → hV$_H$DJ$_H$ (VD-VDJ hybrids)
i) with hV$_H$4-59 footprint (standard VD-VDJ hybrids)
CH103 UCA HCDR3 (13aa)
IGHD3-16*01
IGHJ4*02
CH103 UCA VH
M7923P6 KIVHB5
mIGHD1-1*01
mCDR3 (23 aa)
ii) without hV$_H$4-59 footprint (VDDJ hybrids; have D-D fusion-type junctions)
CH103 UCA HCDR3 (13aa)
CH103 UCA VH
M7913P2 KIVHB5
mIGHD2-2*01
mCDR3 (22 aa)
C
HCDR3
IGHV4-59*01
IGHD3-16*01
IGHJ4*02
---TGACCGCTGCGGACACGGCCGTGTATTACTGTGCGAGCCTGCCCAGGGGGCAGTTAGTCAATGCCTACTTTGACTACTGG---
Cryptic heptamer
Canonical 5' D heptamer CACTGTG
D
Ig site-targeted locus
WT locus
Knocked-in CH103 UCA V$_H$DJ$_H$ rearrangement
CH103 UCA V$_H$DJ$_H$
Cryptic heptamer
Atypical HC rearrangements
V$_H$ replacement
Mouse V$_H$
D
"footprint"
VDVDJ hybrid (with "footprint")
VDDJ hybrid (DD-like fusion; lost "footprint")
Typical (1°) VDJ rearrangements
Atypical (2°) HC rearrangements
primary V->DJ rearrangement
V$_H$ replacement
VDDJ hybrid (with DD fusion)
D->DJ rearrangement (DD fusion via atypical "12-12"recombination
V->DDJ rearrangement (standard "12-23" recombination)
Recombination signal Sequences (RSS):
With a 23bp spacer
With a 12bp spacer

Figure S4. The mechanisms of atypical HC rearrangement-generated hybrid products preferentially expressed by memory IgG$^+$ B-cells of CH505-immunized CH103 homozygous "HC only" KI mice (Related to Figure 3F and Table S2).

Shown are representative examples of the three types of hybrid products formed, with nucleotide sequence alignments of HCDR3s and flanking regions of the knocked-in CH103 UCA HC rearrangement hV_H4-59 / hD3-16 / hJ_H4 (blue lettering) shown relative to the inserted mouse V_H and/or D regions (red lettering). Nucleotide differences in the murine V_H1-22 region relative to human V_H4-59 are shown in colored letters, the block of colored letters (indicated by a **red box**) represents the additional 3' end of mouse V_H1-22, and the string of colored letters 3 of this indicate putative N and/or P nucleotide additions.

(A) Representative example of a mV-hVDJ hybrid product formed as a result of V_H replacement, resulting in a 17 aa (51 bp) HCDR3 replacing the original 13aa (39bp) HCDR3 from the knocked-in CH103 UCA.

(B) Representative example of the two types of mVD-hVDJ hybrid products formed, either: i) a 24aa HCDR3-bearing hybrid with a residual hV_H4-59 footprint, which is found right after the cryptic heptamer embedded in the 3' region of hV_H4-59 (see **C-D**), or ii) a 22aa HCDR3-bearing hybrid, with most of this footprint removed by N and/or P additions (indicated by the **navy blue box**). Since such products that lack obvious footprints normally occur only 28% of the time (Koralov et al., 2006), but are found in our study in 75% of such hybrids (see **Table S2**), and in ~1/3 of all memory IgG+ clones from immunized animals (see **Fig 3F**), this suggests strong vaccine-induced selection for such products.

(C) Nucleotide sequence of the knocked-in CH103 UCA HC rearrangement (hV_H4-59 / hD3-16 / hJ_H4) HCDR3 and flanking regions. Underlined in cyan is the cryptic heptamer embedded at the 3' end of human V_H4-59 (as is found in many human V_H families), with the canonical cryptic heptamer sequence shown below for comparison (Chen et al., 1995). Underlined in navy blue is the 13 aa (39 bp) HCDR3 of the CH103 UCA Ab. The **navy blue box** shows portion of 3' footprint removed by N and/or P additions in the 22 aa VDDJ-resembling hybrids **(D**), originally generated by a RAG-mediated recombination event between an upstream mouse V_H (or a mouse V_HD) and the cryptic heptamer embedded in the 3' end of human V_H4-59 (see below).

(D) Mechanisms by which atypical HC rearrangements at the Ig-site directed locus of KI strains like CH103 UCA HC only mice (left, in red shaded box), or for comparison, those that would normally happen at an untargeted WT locus, including in humans, (right, in blue shaded box). For the former, this includes formation of VD-VDJ hybrids, including both DD fusion-like and standard VD-VDJ hybrids, i.e not retaining (all or most of) or retaining the full 3' hVh4-59 footprint at the site-targeted locus of CH103 UCA "HC only" KI mice, respectively. Note than an intermediate mD->hV_HDJ_H hybrid event is arbitrarily shown at the KI locus, but an alternative intermediate event could be an mV_H->mD recombination product, prior to recombination with the cryptic hV_H39 heptamer. At both types of loci, V_H replacements can be made, whereas VD-VDJ hybrids cannot, due to additional D segments normally being removed after the primary VDJ rearrangement.

Importantly however, VDDJ hybrids (depending on length, either which lose a portion, most or even all of the 3' VH4-59 footprint (the latter like in the mAbs shown in Fig 6A producing DD fusion-resembling products) can also be made at the WT locus, albeit by a different mechanism involving rare (<1000 less efficient) rearrangement of two D segments using their 12bp spacer RSS, thus violating the 12-23bp rearrangement rule of Recombination Signal Sequence (RSS) recombination (Alt et al., 1992). The latter type of standard (primary) VDJ rearrangement events with 12 and 23-spacer-containing RSS are also shown at the top of the WT locus diagram, for comparison.

SUPPLEMENTAL REFERENCES

Alam, S.M., Aussedat, B., Vohra, Y., Ryan Meyerhoff, R., Cale, E.M., Walkowicz, W.E., Radakovich, N.A., Anasti, K., Armand, L., Parks, R.*, et al.* (2017). Mimicry of an HIV broadly neutralizing antibody epitope with a synthetic glycopeptide. Science translational medicine *9*.

Alt, F.W., Oltz, E.M., Young, F., Gorman, J., Taccioli, G., and Chen, J. (1992). VDJ recombination. Immunology today *13*, 306-314.

Chen, C., Nagy, Z., Prak, E.L., and Weigert, M. (1995). Immunoglobulin heavy chain gene replacement: a mechanism of receptor editing. Immunity *3*, 747-755.

Chen, Y., Zhang, J., Hwang, K.K., Bouton-Verville, H., Xia, S.M., Newman, A., Ouyang, Y.B., Haynes, B.F., and Verkoczy, L. (2013). Common tolerance mechanisms, but distinct cross-reactivities associated with gp41 and lipids, limit production of HIV-1 broad neutralizing antibodies 2F5 and 4E10. Journal of immunology *191*, 1260-1275.

de Taeye, S.W., Ozorowski, G., Torrents de la Pena, A., Guttman, M., Julien, J.P., van den Kerkhof, T.L., Burger, J.A., Pritchard, L.K., Pugach, P., Yasmeen, A.*, et al.* (2015). Immunogenicity of Stabilized HIV-1 Envelope Trimers with Reduced Exposure of Non-neutralizing Epitopes. Cell *163*, 1702-1715.

Havenar-Daughton, C., Reiss, S.M., Carnathan, D.G., Wu, J.E., Kendric, K., Torrents de la Pena, A., Kasturi, S.P., Dan, J.M., Bothwell, M., Sanders, R.W.*, et al.* (2016). Cytokine-Independent Detection of Antigen-Specific Germinal Center T Follicular Helper Cells in Immunized Nonhuman Primates Using a Live Cell Activation-Induced Marker Technique. Journal of immunology *197*, 994-1002.

Hulot, S.L., Korber, B., Giorgi, E.E., Vandergrift, N., Saunders, K.O., Balachandran, H., Mach, L.V., Lifton, M.A., Pantaleo, G., Tartaglia, J.*, et al.* (2015). Comparison of Immunogenicity in Rhesus Macaques of Transmitted-Founder, HIV-1 Group M Consensus, and Trivalent Mosaic Envelope Vaccines Formulated as a DNA Prime, NYVAC, and Envelope Protein Boost. Journal of virology *89*, 6462-6480.

Koralov, S.B., Novobrantseva, T.I., Konigsmann, J., Ehlich, A., and Rajewsky, K. (2006). Antibody repertoires generated by VH replacement and direct VH to JH joining. Immunity *25*, 43-53.

Kwon, Y.D., Pancera, M., Acharya, P., Georgiev, I.S., Crooks, E.T., Gorman, J., Joyce, M.G., Guttman, M., Ma, X., Narpala, S.*, et al.* (2015). Crystal structure, conformational fixation and entry-related interactions of mature ligand-free HIV-1 Env. Nature structural & molecular biology *22*, 522-531.

Li, M., Gao, F., Mascola, J.R., Stamatatos, L., Polonis, V.R., Koutsoukos, M., Voss, G., Goepfert, P., Gilbert, P., Greene, K.M.*, et al.* (2005). Human

immunodeficiency virus type 1 env clones from acute and early subtype B infections for standardized assessments of vaccine-elicited neutralizing antibodies. Journal of virology *79*, 10108-10125.

Liao, H.X., Levesque, M.C., Nagel, A., Dixon, A., Zhang, R., Walter, E., Parks, R., Whitesides, J., Marshall, D.J., Hwang, K.K.*, et al.* (2009). High-throughput isolation of immunoglobulin genes from single human B cells and expression as monoclonal antibodies. Journal of virological methods *158*, 171-179.

Liao, H.X., Lynch, R., Zhou, T., Gao, F., Alam, S.M., Boyd, S.D., Fire, A.Z., Roskin, K.M., Schramm, C.A., Zhang, Z.*, et al.* (2013). Co-evolution of a broadly neutralizing HIV-1 antibody and founder virus. Nature *496*, 469-476.

Liu, M., Yang, G., Wiehe, K., Nicely, N.I., Vandergrift, N.A., Rountree, W., Bonsignori, M., Alam, S.M., Gao, J., Haynes, B.F.*, et al.* (2015). Polyreactivity and autoreactivity among HIV-1 antibodies. Journal of virology *89*, 784-798.

Saunders, K.O., Nicely, N.I., Wiehe, K., Bonsignori, M., Meyerhoff, R.R., Parks, R., Walkowicz, W.E., Aussedat, B., Wu, N.R., Cai, F.*, et al.* (2017). Vaccine Elicitation of High Mannose-Dependent Neutralizing Antibodies against the V3-Glycan Broadly Neutralizing Epitope in Nonhuman Primates. Cell reports *18*, 2175-2188.

Shen, X., Basu, R., Sawant, S., Beaumont, D., Kwa, S.F., LaBranche, C., Seaton, K.E., Yates, N.L., Montefiori, D.C., Ferrari, G.*, et al.* (2017). HIV-1 gp120 Protein and MVAgp140 Boost Immunogens Increase immunogenicity of a DNA/MVA HIV-1 Vaccine. Journal of virology.

Tang, G., Peng, L., Baldwin, P.R., Mann, D.S., Jiang, W., Rees, I., and Ludtke, S.J. (2007). EMAN2: an extensible image processing suite for electron microscopy. Journal of structural biology *157*, 38-46.

Verkoczy, L., Chen, Y., Bouton-Verville, H., Zhang, J., Diaz, M., Hutchinson, J., Ouyang, Y.B., Alam, S.M., Holl, T.M., Hwang, K.K.*, et al.* (2011). Rescue of HIV-1 broad neutralizing antibody-expressing B cells in 2F5 VH x VL knockin mice reveals multiple tolerance controls. Journal of immunology *187*, 3785-3797.

Verkoczy, L., Diaz, M., Holl, T.M., Ouyang, Y.B., Bouton-Verville, H., Alam, S.M., Liao, H.X., Kelsoe, G., and Haynes, B.F. (2010). Autoreactivity in an HIV-1 broadly reactive neutralizing antibody variable region heavy chain induces immunologic tolerance. Proceedings of the National Academy of Sciences of the United States of America *107*, 181-186.

Williams, W.B., Zhang, J., Jiang, C., Nicely, N.I., Fera, D., Luo, K., Moody, M.A., Liao, H.X., Alam, S.M., Kepler, T.B.*, et al.* (2017). Initiation of HIV neutralizing B cell lineages with sequential envelope immunizations. Nature communications *8*, 1732.

Zhou, T., Doria-Rose, N.A., Cheng, C., Stewart-Jones, G.B.E., Chuang, G.Y., Chambers, M., Druz, A., Geng, H., McKee, K., Kwon, Y.D.*, et al.* (2017). Quantification of the Impact of the HIV-1-Glycan Shield on Antibody Elicitation. Cell reports *19*, 719-732.